APPLIED PHYSICS LETTERS 104, 032401 (2014)

Antiferromagnetic/ferromagnetic nanostructures for multidigit storage units

R. Morales,[1,2,a)] M. Kovylina,[3] Ivan K. Schuller,[4] A. Labarta,[3] and X. Batlle[3]
[1]*Department of Chemical-Physics, BCMaterials, University of the Basque Country UPV/EHU, 48940 Leioa, Spain*
[2]*IKERBASQUE, Basque Foundation for Science, 48011 Bilbao, Spain*
[3]*Departament de Física Fonamental and Institut de Nanociència i Nanotecnologia, Universitat de Barcelona, 08028 Barcelona, Catalonia, Spain*
[4]*Department of Physics and Center for Advanced Nanoscience, University of California San Diego, La Jolla, California 92093, USA*

(Received 31 October 2013; accepted 20 December 2013; published online 21 January 2014)

The pursuit of higher densities in binary storage media is facing serious operating limitations. In order to overcome these constraints, several multistate techniques have been investigated as alternatives. Here, we report on an approach to define multistate switching memory units based on magnetic nanostructures exhibiting exchange bias. Writing and reading conditions were studied in patterned antiferromagnetic/ferromagnetic thin films. We establish the necessary and sufficient requirements for this multidigit memory concept that might open up new possibilities for the exploration and design of suitable room temperature spintronic devices. © *2014 AIP Publishing LLC*. [http://dx.doi.org/10.1063/1.4862317]

The ever-increasing demand of storage capacity in electronic devices as hard drives and non-volatile solid state memories has pushed the bit feature size to critical limits. Limitations, such as the existence of a minimum volume for a magnetic bit due to superparamagnetic fluctuations,[1,2] high spin-torque current required for the magnetization switching of spin-transfer torque random access memories,[3] micrometer-sized filament formation and leakage currents in resistance switching memories,[4–6] polycrystalline structure in tunnel metal-oxide-semiconductor charge storage cells,[7] thermal fatigue of phase-change memory materials,[8] fluctuations of storing charges in floating-gate cells,[9] scaling constrictions in the manufacturing process,[10] and so on, compromise the miniaturization of binary unit cells of electronic products. In order to overcome these restrictions and increase the storage capacity, more capable mechanisms holding information in multistate digital elements (multidigits) have been proposed. Comparing with the two possible states "0" and "1" of a conventional binary digit (bit), a multidigit memory possesses multiple states which are steady enough to retain written information. For example, while up to 256 characters or numbers (2^8) can be encoded in a sequence of 8 bits, the same sequence of digits with five defined states each one can store up to 390 625 characters (5^8), that is, over 1500 times more than with binary digits. In general, units with N well-defined states can provide up to N^p combinations in a sequence of p multidigit units. Achieving multidigit storage is still a great challenge and different multistate switching techniques have been investigated for the next-generation of high density storage media including magnetic domain walls and vortex states,[11,35] organic thin-film field-effect transistors with memory effect,[12] nonlocal spin valve structure,[13] semiconducting nanowires,[14,15] graphene nanostructures,[16,17] magnetic tunnel junctions,[18,19] local conductivity induced by scanning force microscopy,[20] and memory capacitors.[21]

In this work, we describe an approach for control of the remanence state of antiferromagnetic/ferromagnetic (AF/FM) nanostructures. This enables the design of multidigit switching elements. The magnetic moment of the nanostructure at zero magnetic field can be tuned at any value between positive and negative saturation magnetization (M_S). Tuning the remanent magnetization can alternatively be achieved in AF/FM bilayers by a demagnetization of the FM above the AFM Néel temperature (T_N), which splits the FM layer into opposite domains.[23,36] However, the control of the remanent state proposed here relies on a different physical mechanism. The FM is always saturated by the cooling field (H_{FC}), and its magnitude controls the fraction of FM M_S at zero field, below the AF T_N. $+M_S$ and $-M_S$ usually define a binary digit, i.e., bits "0" and "1," but a fractional M_S ratio would enable more than two states in the same unit. In AF/FM bilayers exhibiting exchange bias, a magnetization hysteresis loop centered about a nonzero magnetic field, H_{EB}, after field cooling, can be set at any remanence state within $\pm M_S$, stable in a wide range of temperature.[22] Such continuous thin films could support magnetic multistates as illustrated in Ref. 23. Loop shifts opposite to [negative exchange bias (NEB)] or along [positive exchange bias (PEB)] the field direction can be generated depending on the magnitude of the cooling field. Each magnetic multistate requires the appropriate external cooling field, H_{FC}, which provides the role of the writing field. Moreover, the magnitude of the writing field can be systematically tuned by lateral patterning of the thin film.[24,25]

AF/FM bilayers (AF = FeF_2, FM = Ni, NiFe, Fe) were prepared by e-beam evaporation on single crystalline MgF_2 (110) as described earlier.[26] FeF_2 becomes AF below the Néel temperature $T_N = 78$ K whilst the FM Curie temperature is well above room temperature. FeF_2 grows epitaxially on MgF_2 and the FM is polycrystalline.[27] For these systems, two important features are essential to define multiple remanence states. First, there must be coexistence of PEB and NEB domains in a range of H_{FC}. Second, both PEB and

a)Electronic mail: rafael.morales@ehu.es

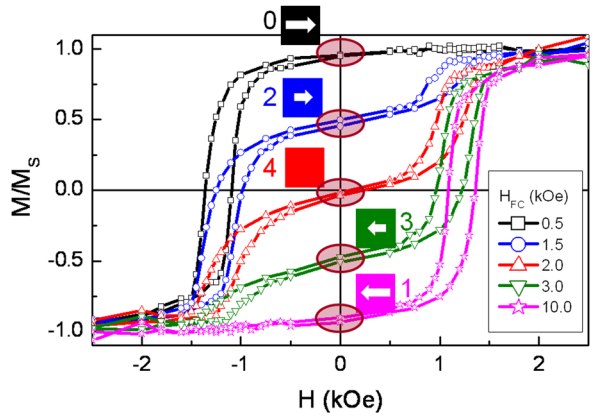

FIG. 1. Hysteresis loops for non-patterned FeF_2 (70 nm)/Ni (20 nm)/Al (4 nm) at five different cooling fields. Remanence states define five digits corresponding to the sketched magnitude and direction of magnetization.

NEB domains must be larger than a certain critical size.[28,29] Both attributes are responsible for the magnetic properties below T_N.

Figure 1 gives an example of the magnetic properties of these thin films showing five magnetic hysteresis loops below T_N for different cooling fields. The MgF_2/FeF_2 (70 nm)/Ni (20 nm)/Al (4 nm) bilayer is saturated above T_N and then the sample is cooled in H_{FC} below T_N. For low H_{FC} (0.5 kOe), a single NEB loop is obtained. The remanence state corresponds to the maximum magnetization, i.e., all spins in the sample are aligned along the positive external field direction. This magnetic state defines the digit 0. The second digit in conventional media, digit 1, corresponds to a spin arrangement with opposite magnetization. This magnetic configuration is achieved by cooling the bilayer below T_N in a high H_{FC} (10 kOe in Figure 1), which yields PEB loops with a full negative remanence. Full PEB requires an antiparallel AF-FM coupling through the interface to take place. Therefore, high enough H_{FC} overcomes the antiparallel interaction between the FM and pinned uncompensated (PUC) AF spins, aligning both net magnetizations parallel during the cooling process. Since AF spins become frozen along the external field direction, the frustrated coupling with FM spins produces the FM magnetization reversal at positive fields.[30,31]

Multiple digits can be written at intermediate H_{FC}. Thus, $H_{FC} = 1.5$ kOe defines digit 2 with half of the full magnetization, whilst $H_{FC} = 3.0$ kOe sets digit 3 with an equivalent magnitude but opposite sign. Digit 4 can be limited to a magnetic state with null magnetization ($H_{FC} = 2.0$ kOe). The intermediate cooling fields produce double hysteresis loops (DHLs), which consist of NEB and PEB subloops separated by a plateau. Stable plateaus of fractional saturation magnetization values are only possible in the "non-averaging" regime.[29] Microscopic fluctuations of the AF-FM coupling give rise to a bidomain state with the coexistence of NEB and PEB domains.[22] For AF domains larger than the FM ones, each FM domain experiences only one sign of interlayer coupling with the same average strength as opposite domains. This "non-averaging" regime yields two subloops with equal absolute magnitude of the exchange bias field (H_{EB}). The domain size ratio between two opposite AF domains, i.e., the remanence of a DHL, is determined by H_{FC}. Higher H_{FC} favors more uncompensated AF spins to be aligned with the external field, which increases the PEB domain size against NEB domains. In this way, a magnetic cell larger than two AF domains can hold multiple digits. The number of digits is limited by the possibility to distinguish different magnetic states, since any remanence value can be obtained by a proper H_{FC}. Note that the relative AF-FM lateral domain size controls the appearance of DHLs. The epitaxial growth of FeF2 assures that we are in the non-averaging regime.

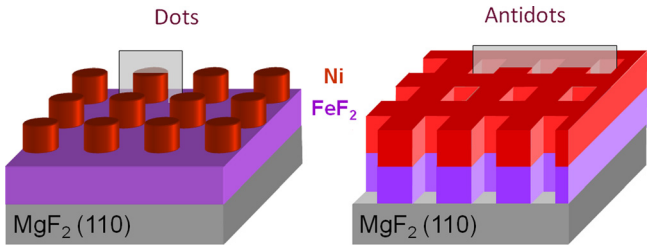

FIG. 2. Illustration of dot and antidot arrays. Dot nanostructures were patterned on the FM only, while antidots were patterned into both the FM and AF layers. Hatch marked areas indicate the cross-section planes of Figure 5, for dots and antidots.

A superior control of multidigit cells can be achieved in patterned media. Multistate storage allows increasing the storage capacity without reducing feature dimensions because in the same area, an increased amount of information can be encoded. Moreover, it has been shown that patterned films into dots or antidots require lower H_{FC} than continuous films to write the same digit.[24,25] This may provide an additional advantage since it can bring the writing field into the useful range.

Figure 2 illustrates the patterned nanostructures, in which the dependence of DHLs on H_{FC} has been investigated. It should be noted that, in the case of circular dots, only the FM layer was patterned, keeping the AF slab as a continuous film, while square antidots were drilled through the full bilayer thickness, creating lateral faces in both the FM and AF materials.

FeF_2/Ni dot arrays were fabricated by electron beam lithography and argon ion milling.[25] Ni dot diameters between

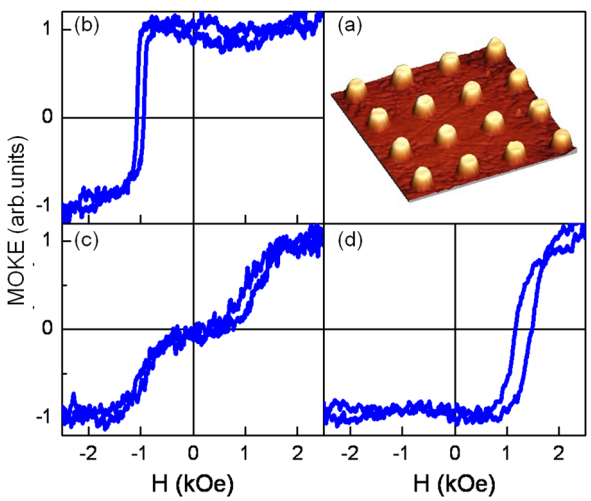

FIG. 3. (a) 4.5 × 4.5 μm^2 AFM image of a FeF_2/Ni dot array. MOKE hysteresis loops for a (b) continuous film (80 × 80 μm^2), (c) 400 nm and (d) 110 nm dot arrays diameter. The cooling field is $H_{FC} = 5$ kOe. The crossover of the loop in (d) at high magnetic fields is due to the experimental error of the technique.

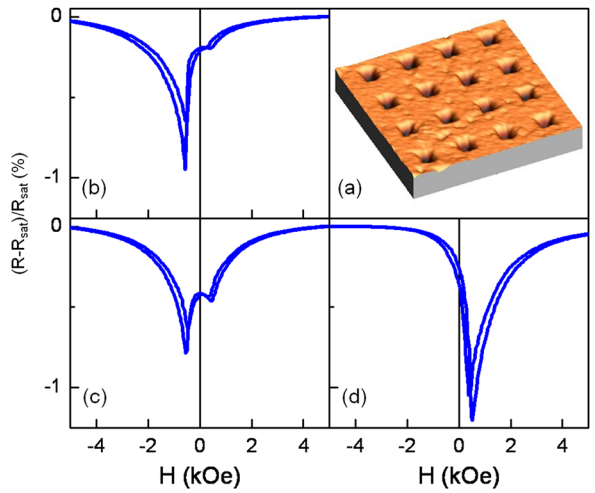

FIG. 4. (a) $2.5 \times 2.5\ \mu m^2$ AFM image of an antidot array in FeF_2/Ni bilayers. Decreasing and increasing magnetic field branches of magnetoresistance curves, $(R(H)-R_{sat})/R_{sat}$, for AD = (b) 0.07, (c) 0.12, and (d) 0.24. The cooling field is $H_{FC} = 2.5$ kOe. $R(H)$ and R_{sat} stand for the resistances at a field H and at the largest applied field, respectively.

110 nm and 700 nm were patterned on FeF_2. Figure 3 shows that the NEB and PEB loops exhibit strong size dependence below T_N. Figure 3(a) shows an atomic force microscopy image of the dot arrays. Figures 3(b)–3(d) show magneto-optical hysteresis loops obtained from a $80 \times 80\ \mu m^2$ unpatterned film, and from arrays of 400 nm and 110 nm dot diameter, respectively. All loops were measured at 10 K for the same cooling field ($H_{FC} = 5$kOe). There is a significant dependence on feature size; the same H_{FC} yields a full NEB loop for the continuous film, a DHL for the 400 nm dots and a full PEB loop for the 110 nm dots. Thus, the external field necessary to write a given digit decreases with feature size. Smaller patterned cells require lower cooling fields for switching multiple remanence states.

A remarkable lateral patterning effect was also found for antidot nanostructures. The magnetic characterization of these patterns was performed by magnetoresistance (MR) measurements that are more sensitive to the local magnetic configuration.[24] Photolithographic masks were used to prepare a series of $10 \times 90\ \mu m^2$ stripes of FeF_2/Ni bilayers and to deposit gold electrodes. Square holes were fabricated by focused ion beam. The edge size was kept constant (200 nm) while the antidot density (AD) was increased from 0.07 to 0.24 (Figure 4(a)).[24,32] Figures 4(b)–4(d) show four-probe electrical resistance measurements for AD = 0.07, 0.12, and 0.24, respectively. All the curves were measured at 4.2 K for the same cooling field, $H_{FC} = 2.5$ kOe. The magnitude of H_{EB} can be extracted from the MR dip positions, at which the transverse component of the magnetization to the current flow is maximum and the electrical resistance is minimum.[33] Patterned antidot arrays show a similar dependence to the dot arrays. A mostly NEB curve is obtained for the lower antidot density (Figure 4(b)), whilst the two minima in Figure 4(c) reveal the coexistence of NEB and PEB with a larger proportion of NEB domains. For the same cooling field, a higher AD density gives rise to a single positively-shifted MR dip, i.e., the sample is in the full PEB state (Figure 4(d)). This result demonstrates that the cooling field necessary for writing multiple digits decreases as the AD density increases.

Thus, we have established that lateral patterning of the AF/FM bilayers has striking effects on the onsets of the DHL and full PEB regimes, and therefore upon the writing fields of multidigits. For both dots and antidots, these effects show similar trends. The smaller the dot diameter or the higher the AD density the lower the cooling field required for writing the same digit. Both findings can be understood within the same picture: the role of the uncompensated spins artificially generated throughout the AF slab by nanostructuring.

Figure 5 illustrates spin configurations yielding full PEB through the cross sections marked in Figure 2 for dots and antidots. Only pinned uncompensated AF spins are colored (compensated spins are not depicted). Blue arrows indicate PUC AF spins coupled to FM moments (gray arrows) at the interface. Red arrows correspond to PUC AF spins not coupled to the FM since they are not in direct contact. These "red" spins have artificially been created during the patterning process on the carved AF faces. All PUC spins (blue and red) depicted in Figure 5 belong to the same AF domain–volume that holds the same sign of EB.[22] Therefore, all of them must be oriented either antiparallel to the FM magnetization (yielding NEB) or parallel to the FM spins (yielding PEB) as in Figure 5.

PEB occurs if during the cooling process the Zeeman energy (E_Z) of PUC AF spins overcomes the exchange energy (E_{ex}) at the AF/FM interface. In this case, uncompensated spins of the AF domain are aligned parallel to the external field. Thus, the Zeeman energy is proportional to the external field, H_{FC}, and the net AF magnetization produced by interfacial spins (blue) and artificially generated spins that are not in direct contact with the FM (red). The exchange energy depends on the AF/FM interfacial area, i.e.,

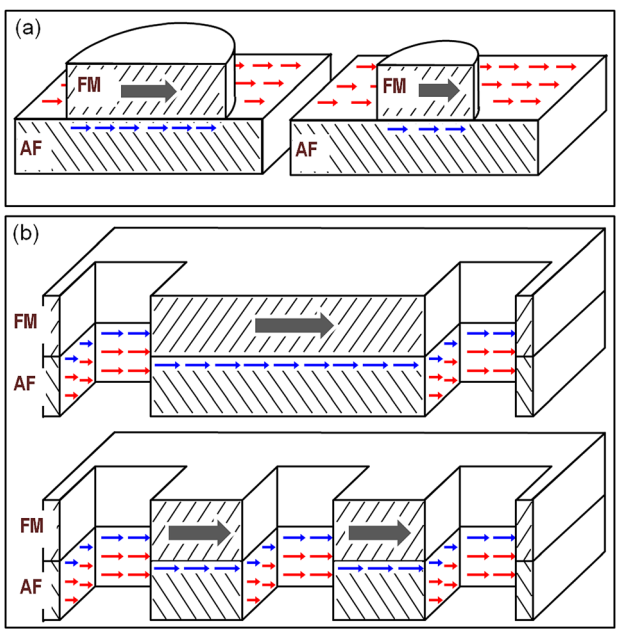

FIG. 5. Cross sections (as marked by hatch marked areas in Fig. 2 for dots and antidots) showing the spin configuration of pinned uncompensated AF moments for a PEB domain. "Blue" arrows represent AF spins at the AF/FM interface. "Red" arrows indicate bare AF spins at exposed AF faces. (a) Two different dot diameters. (b) Two different antidot densities (wide gray arrows indicate the FM magnetization direction).

the number of PUC AF spins at the interface. Therefore, the condition for PEB is

$$E_Z^{in+nc} > E_{ex}^{in},$$

where the superscripts *in* and *nc* refer to interfacial (blue) and non-contact (red) AF spins, respectively. Notice that FM spins play no role in the energy balance since the FM is always saturated under the external H_{FC} for both NEB and PEB.

The interfacial area decreases with the FM dot size, reducing therefore the exchange energy. However, the Zeeman energy that involves both interfacial and non-contact spins remains the same (Figure 5(a)). Thus, a lower cooling field can be applied to overcome E_{ex}^{in}. For antidots, a higher AD generates more non-contact spins on the exposed AF faces carved in the holes (Figure 5(b)), which contribute to the Zeeman energy but not to the exchange energy. Consequently, E_Z increases with respect to E_{ex}, favoring PEB at lower cooling fields.

Recording technology involves two different processes, writing and reading. In this multidigit system, there is only a single writing process: applying H_{FC} above T_N to define the magnetic digit below T_N. However, the digit readout can be performed by either using magnetometry or electrical resistance. Different remanence states of patterned nanostructures could be detected by local magneto-optical Kerr effect (MOKE) or miniaturized superconducting quantum interference device (SQUID) circuitry. These methods might be suitable for magnetic storage media. For non-volatile random access memories, electrical measurement is the common readout procedure. However, the resistance readout of magnetic multistate cells is not sensitive enough to the spin arrangement at remanence. The MR curves do not show a distinguishable plateau around $H = 0$ for NEB, PEB, or DHLs, and the resistance values might not distinguish different digits (Figure 4). The greatest MR variation between different digits is obtained around H_{EB}, where the MR minima appear. Thus, if the readout is performed at $H = +H_{EB}$ the resistance varies from the maximum value for digit 0 (full NEB) to the minimum one for digit 1 (full PEB) (Figures 4(b) and 4(d)). Multiple digits can be defined for resistance values in between corresponding to intermediate cooling fields.[34] Using these multidigit cells as resistance random access memory (RRAM) requires, therefore, an external field for the reading process but this field does not affect the stability of the stored digits around $H = 0$.

In conclusion, this work presents a proof of concept on how magnetic multidigit units can be defined and controlled in patterned magnetic nanostructures with exchange bias. The main requisite is the coexistence of NEB and PEB domains yielding double hysteresis loops. Patterning allows a control of writing fields and design of multistate cells for memory units. Although multidigit ability has been demonstrated in a low temperature AF/FM system, this finding establishes necessary and sufficient conditions which allows extending these results to room temperature magnetic systems. This also shows the capability of exchange coupled nanostructures as a potential multidigit system, and opens new possibilities in AF/FM thin films and synthetic AF multilayers where antiparallel coupling can be attained through a non-magnetic spacer via indirect interaction.

We thank Z.-P. Li for the support in the initial stages of this research. This work was supported by Spanish MICINN and MINECO (FIS2008-06249, MAT2009-0667, and MAT2012-33037), Catalan DURSI (2009SGR856), European Union FEDER funds (Una manera de hacer Europa), UPV/EHU UFI11/23, the 7th European Union Framework Programme (FP7-PEOPLE-2012-IRSES, Project No. 318901), and the US-DOE grant number DE FG03-87ER-45332. XB acknowledges the financial support of the University of Barcelona.

[1]J. Eisenmenger and I. K. Schuller, Nature Mater. **2**, 437 (2003).
[2]V. Skumryev, S. Stoyanov, Y. Zhang, G. Hadjipanayis, D. Givord, and J. Nogués, Nature **423**, 850 (2003).
[3]R. Sbiaa, R. Law, S. Y. H. Lua, E. L. Tan, T. Tahmasebi, C. C. Wang, and S. N. Piramanayagam, Appl. Phys. Lett. **99**, 092506 (2011).
[4]S. H. Jo and W. Lu, Nano Lett. **8**, 392 (2008).
[5]H. K. Lau and C. W. Leung, J. Appl. Phys. **104**, 123705 (2008).
[6]A. Beck, J. G. Bednorz, C. Gerber, C. Rossel, and D. Widmer, Appl. Phys. Lett. **77**, 139 (2000).
[7]T. Z. Lu, M. Alexe, R. Scholz, V. Talelaev, and M. Zacharias, Appl. Phys. Lett. **87**, 202110 (2005).
[8]B. Qiao, J. Feng, Y. Lai, Y. Cai, Y. Lin, T. Tang, B. Cai, and B. Chen, J. Electron. Mater. **36**, 88 (2007).
[9]C.-H. Shih and J.-T. Liang, IEEE Trans. Electron Devices **57**, 1774 (2010).
[10]J. I. Martín, J. Nogués, K. Liu, J. L. Vicent, and I. K. Schuller, J. Magn. Magn. Mater. **256**, 449 (2003).
[11]D. Atkinson, D. S. Eastwood, and L. K. Bogart, Appl. Phys. Lett. **92**, 022510 (2008).
[12]Y. Guo, C. Di, S. Ye, X. Sun, J. Zheng, Y. Wen, W. Wu, G. Yu, and Y. Liu, Adv. Mater. **21**, 1954 (2009).
[13]T. Kimura and M. Hara, Appl. Phys. Lett. **97**, 182501 (2010).
[14]J. I. Sohn, S. S. Choi, S. M. Morris, J. S. Bendall, H. J. Coles, W.-K. Hong, G. Jo, T. Lee, and M. E. Welland, Nano Lett. **10**, 4316 (2010).
[15]K. Nagashima, T. Yanagida, K. Oka, M. Taniguchi, T. Kawai, J.-S. Kim, and B. H. Park, Nano Lett. **10**, 1359 (2010).
[16]C. He, Z. Shi, L. Zhang, W. Yang, R. Yang, D. Shi, and G. Zhang, ACS Nano **6**, 4214 (2012).
[17]J. K. Park, S. M. Song, J. H. Mun, and B. J. Cho, Nano Lett. **11**, 5383 (2011).
[18]P. Krzysteczko, G. Reiss, and A. Thomas, Appl. Phys. Lett. **95**, 112508 (2009).
[19]J. P. Velev, C.-G. Duan, J. D. Burton, A. Smogunov, M. K. Niranjan, E. Tosatti, S. S. Jaswal, and E. Y. Tsymbal, Nano Lett. **9**, 427 (2009).
[20]C. Moreno, C. Munuera, S. Valencia, F. Kronast, X. Obradors, and C. Ocal, Nano Lett. **10**, 3828 (2010).
[21]S. Park, Y.-K. Cha, D. Cha, Y. Park, I.-K. Yoo, J.-H. Lee, K. S. Seol, and S.-H. Choi, Appl. Phys. Lett. **89**, 033122 (2006).
[22]O. Petracic, Z.-P. Li, I. V. Roshchin, M. Viret, R. Morales, X. Batlle, and I. K. Schuller, Appl. Phys. Lett. **87**, 222509 (2005).
[23]I. V. Roshchin, O. Petracic, R. Morales, Z.-P. Li, X. Batlle, and I. K. Schuller, U.S. patent 7,764,454 (July 27, 2010).
[24]M. Kovylina, M. Erekhinsky, R. Morales, J. E. Villegas, I. K. Schuller, A. Labarta, and X. Batlle, Appl. Phys. Lett. **95**, 152507 (2009).
[25]Z.-P. Li, R. Morales, and I. K. Schuller, Appl. Phys. Lett. **94**, 142503 (2009).
[26]R. Morales, Z.-P. Li, O. Petracic, X. Batlle, I. K. Schuller, J. Olamit, and K. Liu, Appl. Phys. Lett. **89**, 072504 (2006).
[27]J. Olamit, E. Arenholz, Z.-P. Li, O. Petracic, I. Roshchin, R. Morales, X. Batlle, I. K. Schuller, and K. Liu, Phys. Rev. B **72**, 012408 (2005).
[28]M. Kovylina, R. Morales, A. Labarta, and X. Batlle, Phys. Rev. B **86**, 224414 (2012).
[29]I. V. Roshchin, O. Petracic, R. Morales, Z.-P. Li, X. Batlle, and I. K. Schuller, Europhys. Lett. **71**, 297 (2005).
[30]S. Roy, M. R. Fitzsimmons, S. Park, M. Dorn, O. Petracic, I. V. Roshchin, Z.-P. Li, X. Batlle, R. Morales, A. Misra, X. Zhang, K. Chesnel, J. B. Kortright, S. K. Sinha, and I. K. Schuller, Phys. Rev. Lett. **95**, 047201 (2005).

[31]M. R. Fitzsimmons, B. J. Kirby, S. Roy, Z.-P. Li, I. V. Roshchin, S. K. Sinha, and I. K. Schuller, Phys. Rev. B **75**, 214412 (2007).
[32]M. Kovylina, M. Erekhinsky, R. Morales, I. K. Schuller, A. Labarta, and X. Batlle, Nanotechnology **21**, 175301 (2010).
[33]T. Gredig, I. N. Krivorotov, and E. D. Dahlberg, J. Appl. Phys. **91**, 7760 (2002).
[34]Note that the MR curves for a fix AD and increasing H_{FC} show the same dependence as in Figures 4(b)–4(d) [see Figure 2 in Ref. 24].
[35]V. Uhlíř, M. Urbánek, L. Hladík, J. Spousta, M.-Y. Im, P. Fischer, N. Eibagi, J. J. Kan, E. E. Fullerton, and T. Sikola, Nature Nanotech. **8**, 341 (2013).
[36]S. Brück, J. Sort, V. Baltz, S. Suriñach, J. S. Muñoz, B. Dieny, M. D. Baró, and J. Nogués, Adv. Mater. **17**, 2978 (2005).